



Rapid detection of genetically modified organisms on a continuous-flow polymerase chain reaction microfluidics

Yuyuan Li, Da Xing*, Chunsun Zhang

MOE Key Laboratory of Laser Life Science and Institute of Laser Life Science, South China Normal University, No. 55, Zhongshan Avenue West, Tianhe District, Guangzhou 510631, People's Republic of China

ARTICLE INFO

Article history:

Received 29 July 2008

Available online 26 October 2008

Keywords:

Polymerase chain reaction

Continuous-flow

Microfluidics

Genetically modified organisms

SYBR Green I

Melting curve analysis

ABSTRACT

The ability to perform DNA amplification on a microfluidic device is very appealing. In this study, a compact continuous-flow polymerase chain reaction (PCR) microfluidics was developed for rapid analysis of genetically modified organisms (GMOs) in genetically modified soybeans. The device consists of three pieces of copper and a transparent polytetrafluoroethylene capillary tube embedded in the spiral channel fabricated on the copper. On this device, the P35S and Tnos sequences were successfully amplified within 9 min, and the limit of detection of the DNA sample was estimated to be 0.005 ng μl^{-1} . Furthermore, a duplex continuous-flow PCR was also reported for the detection of the P35S and Tnos sequences in GMOs simultaneously. This method was coupled with the intercalating dye SYBR Green I and the melting curve analysis of the amplified products. Using this method, temperature differences were identified by the specific melting temperature values of two sequences, and the limit of detection of the DNA sample was assessed to be 0.01 ng μl^{-1} . Therefore, our results demonstrated that the continuous-flow PCR assay could discriminate the GMOs in a cost-saving and less time-consuming way.

© 2008 Elsevier Inc. All rights reserved.

Since the beginning of recombinant DNA technology, genetically modified organisms (GMOs)¹ have brought many advantages such as considerable improvement in the yield and quality of crops and enhancement of the nutritional quality of plants [1]. With the widespread use of GMOs in food production, labeling regulations have been established in some countries to protect the rights of consumers, producers, and retailers [2]. For example, the European Union has been regulating the labeling of genetically modified (GM) foods since 1997 (regulation 258/97/EC).

To verify compliance with labeling requirements, several systems for the detection of GMOs have already been developed and described [3]. Up to now, the detection molecules of GMOs have included DNAs, RNAs, and proteins [4–6]. DNA is a relatively stable molecule, allowing its extraction from all kinds of tissues due to uniqueness of DNA in every type of cell and its analysis from pro-

cessed and heat-treated food products. Therefore, polymerase chain reaction (PCR) [7] based on detection of DNA is the most widespread method [8,9]. For example, the matrix approach proposed by INRA (French National Institute for Agriculture Research) in 1999 for the GMOchips program was a combination of PCR and hybridization to detect authorized and unauthorized GMOs [10]. Currently, a large number of GMOs share the same promoter of the subunit 35S of ribosomal RNA of cauliflower mosaic virus (P35S) and the nopaline synthetase terminator (Tnos) from *Agrobacterium tumefaciens* [11]. Thus, in practice, they are widely amplified to detect whether the tissues contain GM components.

Today most PCR amplifications are carried out on a conventional PCR machine using a heating/cooling block of large heat capacity that often has a number of technical frailties and ultimately restricts the speed and efficiency of the amplification process [12–15]. For rapid PCR, the low heat capacity of the entire PCR system is important, and performing the rapid PCR is difficult in a conventional PCR instrument using a heating/cooling block of large capacity. Therefore, some research groups have made an attempt to develop microfluidics-based PCR biomicrofluidic devices [16,17]. Currently, there are two formats of microfluidic PCR devices [18–20]: microchamber stationary PCR and continuous-flow PCR. The former is the miniaturization of conventional PCR in nature where the PCR mixture is stationary in the chamber and the temperature is cycled repeatedly [21–23]. However, the chamber stationary PCR microfluidics lacks the flexibility to change the

* Corresponding author. Fax: +86 20 85216052.

E-mail address: xingda@scnu.edu.cn (D. Xing).

¹ Abbreviations used: GMO, genetically modified organism; GM, genetically modified; PCR, polymerase chain reaction; P35S, 35S promoter; Tnos, the nopaline synthetase terminator; μ -TAS, micro total analytical system; MCA, melting curve analysis; PID, proportional/integral/derivative; PTFE, polytetrafluoroethylene; dNTP, deoxynucleotide triphosphate; ddH₂O, doubly deionized H₂O; BSA, bovine serum albumin; BPB, bromophenol blue; EDTA, ethylenediaminetetraacetic acid; CV, coefficient of variation; SD, standard deviation; SVR, surface-to-volume ratio; LOD, limit of detection; ELISA, enzyme-linked immunosorbent assay; RT-PCR, real-time PCR.

reaction rate, resulting in more cycling and heating time. Moreover, to reduce the reaction time and power consumption, the system thermal mass must be optimized considerably [24]. Compared with microchamber stationary PCR, the continuous-flow PCR has a few advantages [25]. The heating and cooling rates for PCR amplification are confined not by the system thermal mass but rather by the flow velocities of PCR mixture in a microchannel, the PCR sample solution does not suffer from large evaporation at high temperatures, it is easier to integrate other analytical elements to develop the micro total analytical system (μ -TAS) [26,27], and this format can realize high-throughput PCR amplification by continuously providing various biological sample plugs that could save much time and labor. Currently, the structural styles of the continuous-flow PCR microfluidics can be divided into three main categories: (i) the serpentine channel continuous-flow PCR [25,28–34], a continuous-flow format that is based on the work of Nakano and coworkers [17] and Kopp and coworkers [28]; (ii) the spiral channel continuous-flow PCR [35–41], which consists of a “circular” arrangement of the three zones to generate the sequence of denaturation, annealing, and elongation; and (iii) the straight channel oscillatory-flow PCR [42–45], a type of flow-through PCR microfluidics that consists of a capillary tube, heater zones, an optical window, and so on.

In complying with ISO/DIS 24276, successive simplex DNA amplification and duplex PCR were used in the study for GMO detection to save considerable time and effort. For the purpose of identifying the 195- and 180-bp sequences simultaneously, melting curve analysis (MCA) was exploited in duplex PCR, which was based on SYBR Green I, an intercalating dye that is widely used [46]. With a high affinity for double-stranded DNA and enhanced fluorescence on DNA binding [47], SYBR Green I offers a good alternative as continuous monitoring of the fluorescence of amplicons along with gradient changes in temperature. That can be used to determine the melting curves of these sequences. Although fluorescence in the SYBR Green I reaction is not sequence specific, it is possible to identify the amplified products by their melting temperature (T_m). Because the melting curve of a product is dependent on GC content, length, and sequence, PCR products can be distinguished by MCA [48].

Materials and methods

Apparatus

The continuous-flow PCR microfluidics device, depicted schematically in Fig. 1, was manufactured by Automation Engineering R&M Centre (AERMC, Guangdong Academy of Sciences, Guangzhou, China). It consists of a 4-cm diameter and 10-cm length copper cylinder machined into three pieces corresponding to the denaturation, annealing, and extension regions. The extension re-

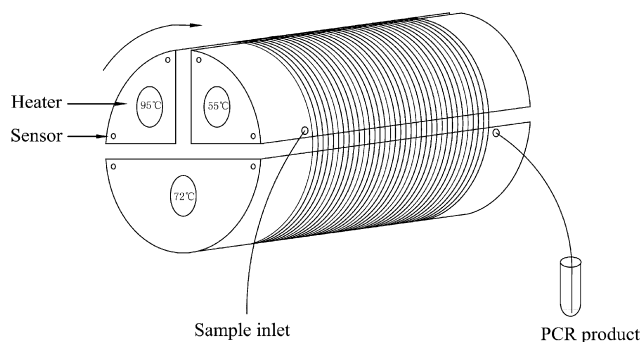


Fig. 1. Schematic diagram of continuous-flow PCR microfluidics.

gion is twice the size of the other two zones. The three temperature zones are separated from each other by thermally insulating sheets that have a thickness of 3 mm. Each zone includes one larger central hole (8 mm diameter) for the resistance cartridge heater (8 mm diameter, 100 mm length, 300 W, Guangzhou Haoyi Thermal Electronics Factory, Guangzhou, China) and two small holes (1 mm diameter and 10 mm depth) for the K-type thermocouples (0.005 inch diameter, Omega Engineering, Stamford, CT, USA). The thermocouples were connected to a data acquisition system (model PCI 4351, National Instruments, Austin, TX, USA) that converted the analog signal to a digital one. To control the temperatures for denaturation at 94 °C, annealing at 56 °C and extension at 72 °C, a computer received the temperature signal through a PCI-4351 interface (National Instruments) and determined the power input to the heater using a homemade fuzzy proportional/integral/derivative (PID) control algorithm that was programmed with LabVIEW 8.0 (National Instruments).

A 5.2-m long transparent polytetrafluoroethylene (PTFE) capillary (0.5 mm i.d./0.9 mm o.d., Wuxi Xiangjian Tetrafluoroethylene Product, Wuxi, China) includes the inlet for samples injection and the outlet for product collection. It enters the cylinder through a hole (1.5 mm diameter) crossing the annealing and denaturation zones, providing an initial denaturation step. Then the capillary is wound 35 cycles in the spiral channel (1.1 mm width and 1.1 mm depth). The capillary exits the cylinder through a hole (1.5 mm diameter) in the elongation region, providing an additional extension on the 35th cycle. The inlet and outlet lengths of the capillary both were approximately 0.35 m. When the PCR cycles were increased to 45, the length of PTFE capillary was changed to 6.5 m. This device can perform up to 60 cycles.

Reagents and samples

PCR reagents, 10 \times Taq DNA polymerase buffer (500 mM KCl and 100 mM Tris-HCl, pH 8.8), MgCl₂ solution (25 mM), and thermostable Taq polymerase (5 U μ l⁻¹) were purchased from Bio Basic (BBI, Ontario, Canada). Deoxynucleotide triphosphates (dNTPs, 10 mM each of dATP, dGTP, dCTP, and dTTP) and PCR primers [11] (Table 1) were obtained from Shanghai Sangon Biological Engineering & Technology Services (SSBE, Shanghai, China). The doubly deionized H₂O (ddH₂O) was provided by Tiangen Biotech (Beijing, China). GM soybeans were gifts from Guangdong Entry-Exit Inspection and Quarantine Bureau (Guangzhou, China), and the genomic DNA of soybean was extracted by using a plant genomic DNA extraction kit (Win Honor Bioscience [South], Guangzhou, China).

Bovine serum albumin (BSA, fraction V, purity \geq 98%, biotechnology grade, cat. no. 735094), which was used to dynamically coat the inner surface to decrease the surface adsorption [25], was purchased from Roche Diagnostics (Mannheim, Germany). Sodium hypochlorite solution, which was used to remove the residual DNA from the microchannel after each of the amplifications, was obtained from Guanghua Chemical Factory (Guangzhou, China). GoldView dye and SYBR Green I were purchased from SBS Genetech (Beijing, China). The DNA markers, which contain 2000-, 1000-, 750-, 500-, 250-, and 100-bp DNA fragments, were obtained from Win Honor Bioscience (South).

Continuous-flow PCR amplification

For the continuous-flow PCR amplification, 25 μ l of PCR mixture consists of 1 \times PCR buffer, 1.5 mM MgCl₂, 0.2 mM of each dNTP, the primer pair (0.5 μ M each), 5 ng μ l⁻¹ soybean genomic DNA, 0.05 U μ l⁻¹ Taq DNA polymerase, and 0.025% (m/v) BSA. The PCR mixture was introduced into the capillary from the inlet and compelled by the precision syringe pump (cat. no. CZ-74901-15, Cole-Parmer

Table 1
Primers used in the study

Name	Sense	Antisense	Amplicon size (bp)
P35S primers	5'-GCTCCTACAATGCCATCA-3'	5'-GATAGTGGGATTGTGCGTCA-3'	195
Tnos primers	5'-GAATCCTGTGCCGGTCTTG-3'	5'-TTATCCTAGTTTGGCGCTA-3'	180

Instrument, Vernon Hills, IL, USA) to flow continuously through the microchannel. The 0.2-ml thin-walled polypropylene tube was used to collect the products and stored at 4 °C for further analysis.

The capillary was to be used for a number of amplification experiments, so a cleaning method was developed to validly remove the residual PCR mixtures from the microchannel. The method consists of a 100- μ l purification wash of 5% sodium hypochlorite solution and a 100- μ l cleaning of deionized water, followed by a 50- μ l rinse of 1 \times PCR buffer.

To compare amplification characteristics (speed, specificity, and yield), the positive control PCR was performed on a conventional PCR apparatus, which was a commercial Mastercycler gradient PCR machine (Eppendorf, Hamburg, Germany). The cycling procedures were set as follows: an initial step of denaturation at 94 °C for 3 min; 35 cycles of denaturation at 94 °C for 30 s, anneal at 55 °C for 30 s, and elongation at 72 °C for 1 min; and final extension at 72 °C for 3 min. In total, the above program requires 85 min. To validate the amplification, negative controls (without template DNA) were also performed to ascertain whether the residual contamination existed. All experiments in this work were repeated three times to verify the accuracy of the experiments.

Continuous-flow PCR at various flow rates

To verify the rapid detection capability of the microfluidic device, PCR of the 195-bp sequence in the P35S and the 180-bp sequence in the Tnos of GM soybeans was performed at different flow rates of the corresponding PCR mixture through the thermal cycling capillary. The flow velocity was controlled by the syringe, ranging from 2.0 to 15.0 mm s⁻¹. The components in the PCR mixture are the same as those mentioned above.

Continuous-flow PCR at various initial DNA concentrations

The continuous-flow PCR was performed using a wide range of DNA concentrations from 0.001 to 7.5 ng μ l⁻¹. The 180-bp sequence was amplified at a flow rate of 3.5 mm s⁻¹, then analyzed by the gel agarose electrophoresis, and amplified at a flow rate of 5.0 mm s⁻¹, then analyzed by melting curves. These experiments were also performed on the conventional PCR machine, which was a commercial Mastercycler gradient PCR machine, and the cycling procedures were the same as the descriptions mentioned above.

Segmented-flow PCR of different DNA samples

PCR mixtures (25 μ l) were prepared with different DNA samples and PCR primers for amplifying the 180-bp sequence and/or 195-bp sequence. Different DNA samples in PCR mixtures included the genomic DNA of GM and non-GM soybeans. Then these PCR mixtures were sequentially injected into the capillary, and the negative control was injected after the PCR mixture containing the genomic DNA of non-GM soybeans, which was amplified to ascertain whether the resulting amplicon was a product of residual contamination. Then these PCR mixtures were driven to flow through the thermal cycling capillary at a flow velocity of 3.5 mm s⁻¹. Between each sample introduced, we interposed small air gaps, 15 μ l of 1 \times PCR buffer containing 0.4 \times bromophenol blue (BPB) buffer, and then small air gaps. This cleaning method was used to effectively

remove the residual DNA from the microchannel, and each PCR product could also be collected separately for further analysis.

Duplex PCR on the continuous-flow device

The PCR mixture (25 μ l) consisted of 1 \times PCR buffer, 1.5 mM MgCl₂, 0.2 mM of each dNTP, 5.0 ng μ l⁻¹ soybean genomic DNA, two pairs of primers (the final concentration of 200 nM for the P35S sequence and 400 nM for the Tnos sequence), 0.1 U μ l⁻¹ Taq DNA polymerase, and 0.05% (m/v) BSA. The flow velocity was controlled at 5 mm s⁻¹ by the syringe. To study the effect of the amount of initial DNA sample on duplex PCR, amplifications were also performed using a wide range of DNA concentrations from 0.005 to 5.0 ng μ l⁻¹.

Analysis of amplification products

Here 8 μ l of each PCR product with 1.6 μ l of 6 \times loading buffer was separated by agarose gel electrophoresis. Loading buffer contained 30 mM ethylenediaminetetraacetic acid (EDTA), 36% (v/v) glycerol, 0.05% (w/v) xylene cyanol FF, and 0.05% (w/v) BPB. The gel was prepared with 1.5% agarose in 0.5 \times TBE buffer containing 0.5 μ l ml⁻¹ GoldView as fluorescence dye. The running conditions were constant voltage at 100 V. After electrophoresis, which took approximately 30 min, the relative amounts of PCR products were analyzed by image analysis software (Quantity One, Bio-Rad, Hercules, CA, USA). The DL 2000 DNA markers, which contain 2000-, 1000-, 750-, 500-, 250-, and 100-bp DNA fragments, were used as standards for the evaluation of the gels.

After continuous-flow PCR, MCA using SYBR Green I was performed with the LightCycler (Roche Diagnostics, Mannheim, Germany). The products with SYBR Green I (1 \times) were heated to 95 °C during 15 s, cooled at 60 °C for 20 s, and then slowly heated back to 95 °C at a rate of 0.1 °C s⁻¹. Obtained fluorescence signals were monitored continuously during the slow warming-up gradient and slowed to a decreasing curve with a sharp fluorescence drop near the denaturation temperature. Plotting the negative derivative of the fluorescence over the temperature versus the temperature ($-dF/dT$ vs. T) generated peaks from which the T_m values of the products were calculated [49].

Results and discussion

Effect of various flow rates on the continuous-flow PCR amplification

The cycling rate of the continuous-flow PCR thermocycler depends, to some extent, on the flow rate of the PCR mixture, the substrate material, and the size of the microchannel [40]. Therefore, an obvious characteristic of the continuous-flow PCR amplification is that thermocycling rates of PCR amplification can be regulated by changing the flow rates of the PCR mixture through the flow channel. The upper panel of Fig. 2A shows the gel electrophoresis results of the 195-bp sequence in P35S obtained at flow rates ranging from 2.0 to 15.0 mm s⁻¹, whereas the lower panel of Fig. 2A shows the relative amounts of obtained PCR products as determined by image analysis software. Values were normalized to the fluorescence of the positive PCR products from the conventional PCR machine (100%, lane 1). With the increase of flow veloc-

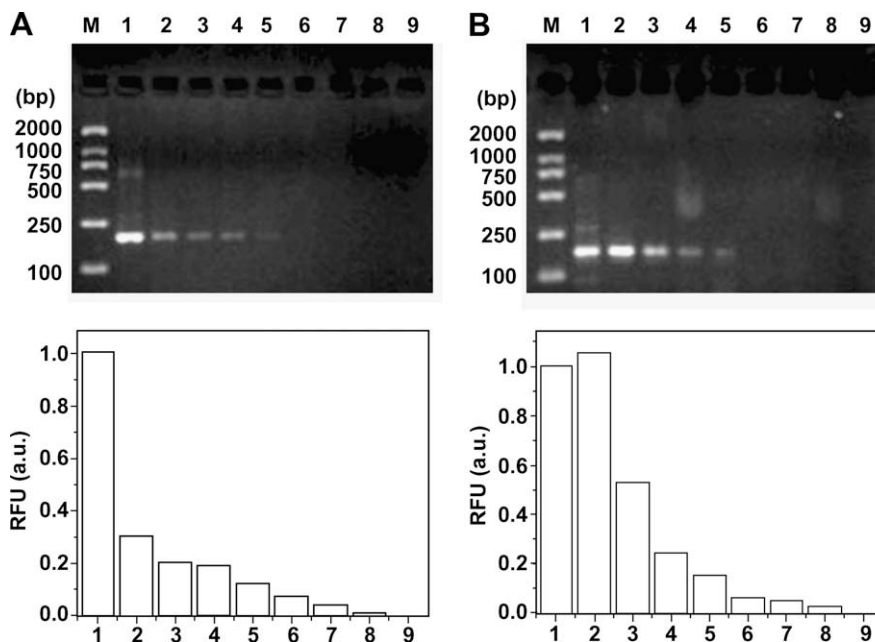


Fig. 2. Effect of the flow rates on the continuous-flow PCR yield. The top panels show fluorescence images of PCR products of the P35S sequence (A) and the Tnos sequence (B) in 1.5% agarose gel. Lane M: DL 2000 marker; lane 1: positive control PCR product from the conventional PCR machine (a commercial Mastercycler gradient PCR machine); lanes 2 to 8: continuous-flow PCR products at flow rates of 2.0, 3.5, 5.0, 7.5, 10.0, 12.5, and 15.0 mm s⁻¹, respectively; lane 9: negative control PCR, PCR mixture solution with no DNA sample run at a flow rate of 5.0 mm s⁻¹. The lower panels show a comparison of band intensities of the respective upper panels that was analyzed by image analysis software (Quantity One). Values were normalized to the fluorescence of the product from the conventional PCR machine (100%, lane 1).

ities, the amount of PCR products is gradually decreased, but the PCR reaction speed is raised gradually. The corresponding times of the PCR mixture flowing through the PTFE capillary range from approximately 40 to 6 min. At a flow rate of 7.5 mm s⁻¹, the PCR products can be detected using only approximately 11 min after 35 cycles (lane 5 in upper panel of Fig. 2A). In addition, the PCR products cannot be easily observed by electrophoresis when the flow rates were increased to 10 mm s⁻¹ or higher (lanes 6–8). This experimental phenomenon was also observed while amplifying the Tnos sequence of GM soybeans at flow rates ranging from 2.0 to 15.0 mm s⁻¹ (Fig. 2B, upper and lower panels). This does not necessarily mean that there were no products obtained at those rates; more likely, it means that the amount of PCR products under these PCR conditions was smaller than the detection limit of the fluorescence scanner associated with the gel imaging system.

However, using the MCA, amplicons can be detected when the flow velocity was increased to 10 mm s⁻¹ (Fig. 3). In other words, the whole continuous-flow PCR might require 9 min and has a successful determination. In addition, MCA requires only approximately 7 min, which obviates the need to examine PCR products on time-consuming agarose gels. After continuous-flow PCR amplification, the LightCycler monitors the decrease of fluorescence resulting from the release of SYBR Green I during DNA melting curve analysis by the slow increase of the temperature. Because the melting curve's shape is dependent on GC content, length, and sequence, the *T_m* of specific amplicons and unique shape of the melting peak can be used to differentiate the target genes and identify them [48]. The average *T_m* (\bar{T}_m) from three independent assays was 78.99 ± 0.24 °C with a coefficient of variation (CV) of 0.30% for the Tnos sequence (180 bp, G + C 32.8%) and 84.60 ± 0.37 °C with a CV of 0.43% for the P35S sequence (195 bp, G + C 50.3%). Test results were considered as positive when the *T_m* was within the \bar{T}_m ± 3 standard deviations (SD) for each sequence [50]. The ranges were from 78.27 to 79.71 °C for Tnos and from 83.49 to 85.71 °C for P35S.

Nevertheless, when the flow rate was raised to 12.5 mm s⁻¹ or higher, no signal of PCR products was detected. Maybe it is because

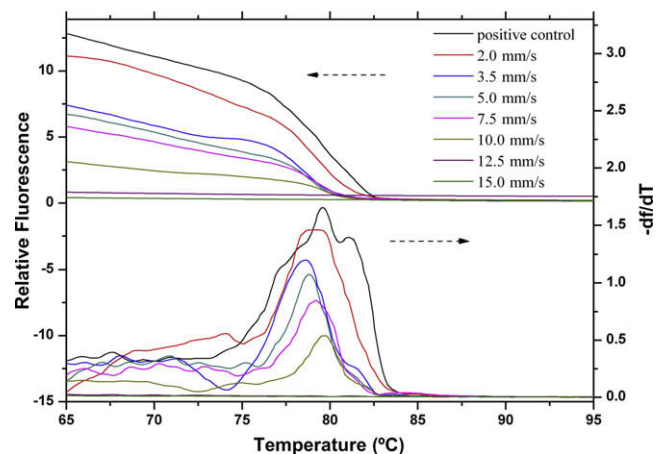


Fig. 3. Fluorescence melting curves for the amplification products of the Tnos sequence on the microfluidic device at various flow rates. The various flow rates of the PCR mixture in the microchannel were 2.0, 3.5, 5.0, 7.5, 10.0, 12.5, and 15.0 mm s⁻¹. The positive control PCR product was from the conventional PCR machine (a commercial Mastercycler gradient PCR machine). After continuous-flow PCR, melting curve analysis was performed with the LightCycler. The products with SYBR Green I were heated to 95 °C during 15 s, cooled at 60 °C for 20 s, and then slowly heated back to 95 °C at a rate 0.1 °C s⁻¹.

the maximal thermal cycling rate of continuous-flow PCR microfluidics is controlled by the dynamics of Taq DNA polymerase, whose extension rate is approximately 60 to 100 bases s⁻¹ at 72 °C [19,25]. In other words, the residence time of PCR mixture in the extension zone was below the kinetic rate of the polymerase enzyme [37]. In addition, it is also affected by the size of the PTFE capillary. The thick-walled PTFE capillary possessing low thermal conductivity will increase the time required to transfer the heat from the outer to the inner of the capillary, and likewise the large diameter of the capillary will reduce the speed of thermal equilibration of the PCR reaction mixture in the capillary channel. It is

worth noting that the amount of the products amplified at a flow rate of 2.0 mm s^{-1} is higher than that of the positive control PCR products from the conventional PCR machine (lane 2 in upper panel of Fig. 2B). This phenomenon may be attributed to the fact that the heating and cooling rates of the microfluidics are higher than those of the conventional PCR, and so the possibility of nonspecific PCR products derived from false priming decreases, thereby enhancing the efficiency of the amplification. Moreover, the results of MCA show that our supposition is reasonable. It is clear that the peak shape of the products amplified on the continuous-flow PCR microfluidics is sharper than that of amplicons from the conventional PCR machine (Fig. 3).

Moreover, to determine that there are no false-positive amplifications by this methodology, amplification using 45 cycles was also performed on this microfluidic device at a flow rate of 5.0 mm s^{-1} (Fig. 4).

Effect of DNA sample concentration on PCR amplification

It is important to study the effect of the amount of initial DNA sample on continuous-flow PCR amplification. Because the surface-to-volume ratio (SVR) of the continuous-flow PCR microfluidics (8 mm^{-1}) is much larger than that of the polypropylene tube (1.5 mm^{-1}) [41], there is a greater possibility of adsorption of biomacromolecules onto the capillary inner surface that may inhibit the PCR amplification. Based on our previous work [41], a flow rate of 3.5 mm^{-1} was chosen in this set of experiments for considering the production and time of amplification. The upper panel of Fig. 5A shows the gel electrophoresis results of the Tnos sequence amplified under the DNA sample concentrations from 7.5 to $0.001 \text{ ng } \mu\text{l}^{-1}$, whereas the lower panel shows the relative amounts of obtained PCR products as determined by image analysis software. Values were normalized to the fluorescence of the products under a DNA sample concentration of $7.5 \text{ ng } \mu\text{l}^{-1}$ (100%, lane 1). It can be seen from the upper panel of Fig. 5A that the yield of PCR products of the Tnos sequence is decreased with the reduction of the DNA sample concentration from 7.5 to $0.001 \text{ ng } \mu\text{l}^{-1}$. The lowest DNA concentration that could be visibly detected by agarose gel electrophoresis is up to $0.05 \text{ ng } \mu\text{l}^{-1}$ (lane 7). Although no visible product band was apparent for the $0.01\text{-ng } \mu\text{l}^{-1}$ DNA sample, this does not necessarily mean that no product was generated at those concentrations; more likely, it means that the amount of products produced under these PCR conditions was smaller than the detection limit of the fluorescence scanner associated with the gel imaging system. Namely, the limit of detection (LOD) of DNA sample that can be used in this continuous-flow PCR device with

electrophoresis detection system is $0.05 \text{ ng } \mu\text{l}^{-1}$. The amount of PCR products under this concentration condition is approximately 10% of the products under a DNA concentration of $7.5 \text{ ng } \mu\text{l}^{-1}$. Comparing the results of experiments in Fig. 2 with those in Fig. 3, it is not hard to see that the sensitivity of the MCA method is higher than that of agarose gel electrophoresis. Therefore, to further enhance the efficiency of amplification, we chose a flow rate of 5.0 mm s^{-1} and then used the MCA for the detection of the Tnos sequence, and the sensitivity is improved to $0.005 \text{ ng } \mu\text{l}^{-1}$ of the DNA concentration (Fig. 6). There is a weak peak when the DNA concentration is reduced to $0.001 \text{ ng } \mu\text{l}^{-1}$. However, the signal-to-noise ratio is relatively low, so it cannot be considered as a positive result. That is, the LOD of the DNA sample that can be used in this continuous-flow PCR device with the MCA detection system is $0.005 \text{ ng } \mu\text{l}^{-1}$.

On the commercial Mastercycler gradient PCR machine, we also detected the Tnos sequence to investigate the effect of the amount of initial DNA sample (Fig. 5B, upper and lower panels). Because the SVR of the polypropylene tube is relatively small, the possibility of adsorption of biomacromolecules onto the tube wall is lower. Therefore, when the DNA concentration is decreased to $0.001 \text{ ng } \mu\text{l}^{-1}$, the PCR product band obtained is also evident.

Successive amplification of different DNA samples

For continuous-flow PCR, one of the important superiorities is that it is very facile to perform successive DNA amplification by using a continuous segmented flow of different PCR mixtures containing different DNA samples. This format of amplification can save time and simplify the operation to a large extent. During recent years, some researchers have studied the successive amplification of different PCR mixtures and the tactics of contamination-free amplification in a continuous-flow format [30,35,36,39]. In the current study, we used a method similar to that referred to in Park and coworkers' work [36] to get rid of the cross-contamination from successive PCR amplification of the Tnos and/or P35S sequences with different samples: GM soybeans, non-GM soybeans, and the negative control. To cleanse the carryover from the preceding segment to the following one, we interposed $1\times$ PCR buffer containing $0.4\times$ BPB buffer between each segment. Due to the fact that the buffer is widely used in loading DNA samples on electrophoresis gels, DNA molecules would dissolve in it very well. Moreover, it is blue, and so each sample segment is easily located and separated. Fig. 7A illustrates the segmented-flow mode of continuous PCR amplification of different DNA samples. Figs. 7B and 7C demonstrate the successive amplification of the Tnos and P35S sequences with three segments of PCR mixtures. Fig. 7D shows the gel electrophoresis results of successive amplification with six segments of PCR mixtures. As shown in Fig. 7, the absence of cross-contamination between samples is demonstrated, and the injection of negative samples before and after a positive sample, as shown in Fig. 7D, confirms that the amplicon was copied from the desired template. The cleaning method was able to reduce the PCR residue between amplifications. The experimental results of the experiments indicate that there is little carryover and inhibition in this system.

This very high-throughput methodology is nearly qualitative and determines the presence or absence of GMOs for each of the samples. It is effectively to control that no such unauthorized GMO exists in commercialized food. Note that some authorized GMOs (e.g., Roundup Ready soy) have been adopted by local regulations, but there is a positive threshold when there are no safety issues. The current European Union regulations (1829/2003/EC and 1830/2003/EC) stipulate that the products in which the GMO contents are more than 0.9% must be labeled. In some cases, the optical density in an enzyme-linked immunosorbent assay (ELISA)

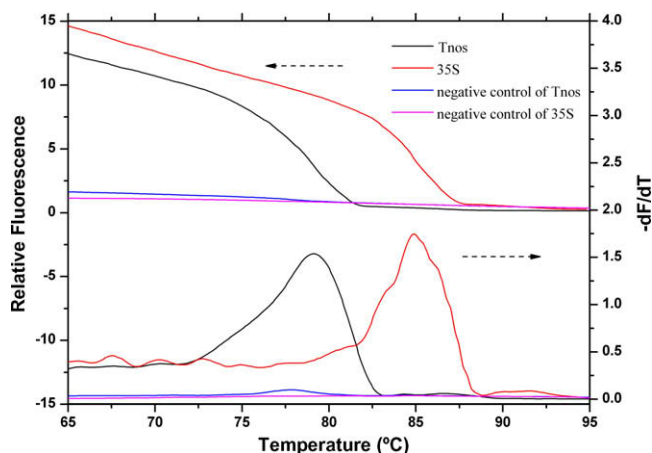


Fig. 4. Fluorescence melting curves for the amplification products of the P35S and Tnos sequences on the microfluidic device using 45 cycles at a flow rate of 5.0 mm s^{-1} .

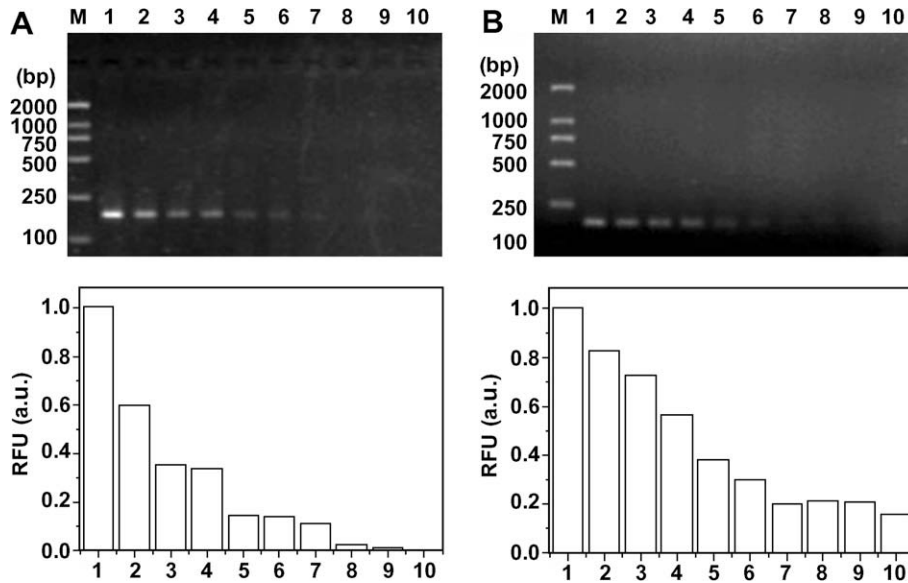


Fig. 5. Fluorescence intensity of the product gel band as a function of the input DNA molecules. The top panels show the DNA sample concentration effect for the amplification of the Tnos sequence on the continuous-flow PCR microfluidics at a flow rate of 3.5 mm s^{-1} (A) and the same effect on the conventional PCR machine (a commercial Mastercycler gradient PCR machine). (B) Lane M: DL 2000 marker; lanes 1 to 10: PCR products from various concentrations of the input DNA molecules (7.5, 5.0, 2.5, 1.0, 0.5, 0.1, 0.05, 0.01, 0.005, and $0.001 \text{ ng } \mu\text{l}^{-1}$, respectively). The lower panels show a comparison of band intensities of the respective upper panels that was analyzed by image analysis software (Quantity One). Values were normalized to the fluorescence of the product under a DNA sample concentration of $7.5 \text{ ng } \mu\text{l}^{-1}$ (100%, lane 1).

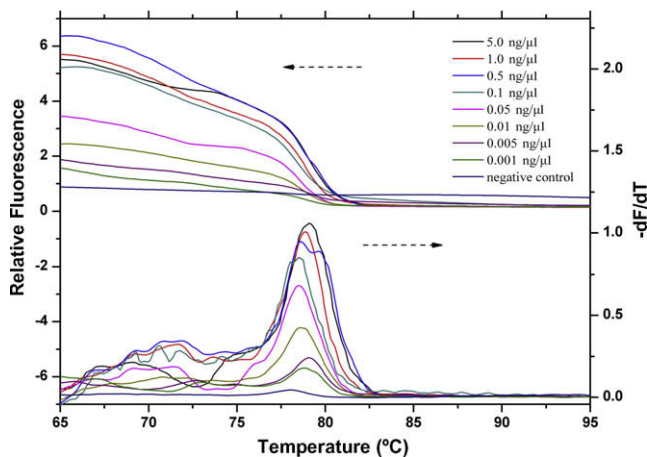


Fig. 6. Fluorescence melting curves for the amplification products of the Tnos sequence on the microfluidic device with the different concentrations of the input DNA molecules. The various concentrations of the input DNA molecules were 5.0, 1.0, 0.5, 0.1, 0.05, 0.01, 0.005, and $0.001 \text{ ng } \mu\text{l}^{-1}$. The negative control PCR was also performed. The amplification was performed at a flow rate of 5.0 mm s^{-1} . Other conditions were as in Fig. 3.

method, the cycle threshold (C_t) in a real-time PCR (RT-PCR), and so on can be calibrated to predict the GMO concentration. But doing that rigorously implies good knowledge of the distribution of the response and its uncertainty. With the method “quality control by attributes” [51,52], this successive amplification in a continuous-flow format can also be quantitative.

Duplex continuous-flow PCR systems based on MCA method

Unlike gel electrophoresis, MCA can distinguish products of the same length but different GC/AT ratios. Assuming that T_m differences above 2°C may allow discrimination of the PCR products, it was easy to differentiate P35S and Tnos sequences with $\overline{T_m}$ values differing by approximately 5.6°C . So, we chose this method for the postamplification detection of the P35S and Tnos sequences,

which cannot be discriminated distinctly after the duplex PCR using agarose gel electrophoresis to identify 15-bp differences. Duplex PCR assay, which simultaneously amplifies the P35S and Tnos sequences in a single PCR, saves significant time and labor compared with individual PCR assays. After a careful analysis of the respective experimental T_m , we optimized the concentrations of primers to perform the duplex amplification for the P35S and Tnos sequences. Each pair of primers was optimized to a final concentration of 200 and 400 nM for the P35S and Tnos sequences, respectively. The concentration of Taq DNA polymerase was $0.1 \text{ U } \mu\text{l}^{-1}$ for the duplex continuous-flow PCR. As shown in Fig. 8, using that concentration of Taq DNA polymerase, P35S and Tnos sequences were amplified in simplex PCR format respectively and simultaneously amplified in duplex PCR. It was possible to unambiguously amplify and identify each fragment in duplex continuous-flow PCR coupled with MCA. In addition, in a comparison with Fig. 3, Fig. 8 illustrates that the PCR efficiency could be improved with an increase of Taq DNA polymerase concentration [25,41].

The LOD of DNA sample of duplex PCR on this microfluidic device was also assessed. It can be seen from Fig. 9 that the sensitivity of duplex PCR detection is estimated to be $0.01 \text{ ng } \mu\text{l}^{-1}$. When the DNA concentration is reduced to $0.005 \text{ ng } \mu\text{l}^{-1}$, there is only a weak peak of the Tnos sequence but not in the temperature range of the T_m of the P35S sequence.

Conclusion

The continuous-flow PCR presented here has been shown to be a new technique for the detection of GMOs. The systems described are highly convenient for use in routine GMO identification analysis. The amplification of the P35S and the Tnos sequences could be successfully completed within approximately 9 min on this compact, spiral, channel-based, continuous-flow PCR microfluidics; thus, the amplification rate was much faster than that of the conventional PCR machine. In addition, the LOD of DNA sample in the presented continuous-flow PCR microfluidics is estimated to be $0.005 \text{ ng } \mu\text{l}^{-1}$. Furthermore, duplex continuous-flow PCR was also reported for the detection of the P35 and Tnos sequences simulta-

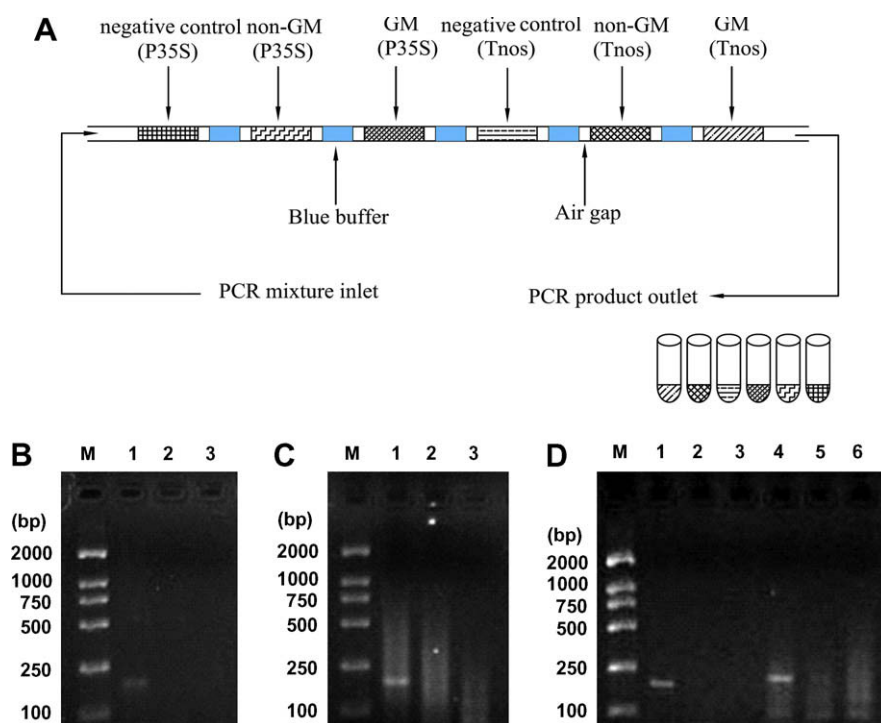


Fig. 7. (A) Segmented-flow mode of continuous PCR amplification of different DNA samples. (B) Successive amplification of Tnos sequence with different DNA samples: GM soybeans, non-GM soybeans, and negative control. (C) Successive amplification of P35S sequence with different DNA samples: GM soybeans, non-GM soybeans, and negative control. (D) Successive amplification of Tnos and P35S sequences with different DNA samples: GM soybeans, non-GM soybeans, and negative control. Lane M: DL 2000 marker; lanes 1 to 3 in panels B and D: sequential amplification of Tnos sequence with different DNA samples: GM soybeans, non-GM soybeans, and negative control, respectively; lanes 1 to 3 in panel C and lanes 4 to 6 in panel D: sequential amplification of P35S sequence with different DNA samples: GM soybeans, non-GM soybeans, and negative control, respectively.

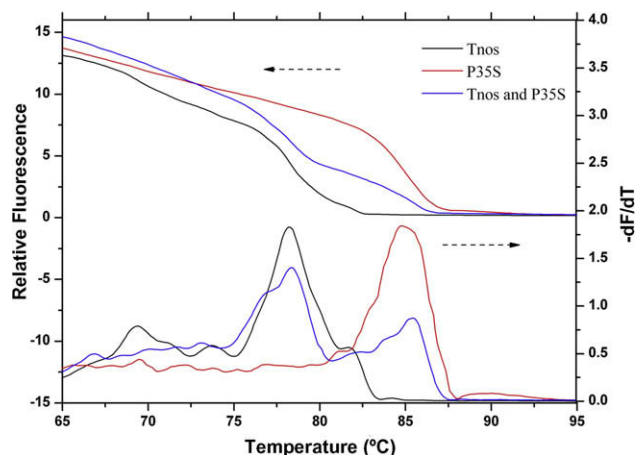


Fig. 8. Melting curve analysis of duplex PCR products on the microfluidic device. The amplification was performed at a flow rate of 5.0 mm s^{-1} . Other conditions were as in Fig. 3.

neously coupled with MCA of the products, and the LOD of DNA sample is assessed to be $0.01 \text{ ng } \mu\text{l}^{-1}$. It should be noted that with continuous-flow PCR it could be very easy to perform successive DNA amplification, which could save time and simplify the operation to a large extent.

This work represents the first step for an automated continuous-flow PCR system for the detection of GMOs, and several further improvements still are required for the automated rapid detection. Those include integration with preamplification processes, such as DNA extraction and sample mixing, and postamplification product detection. On-line sample preparation is superior in speed and sample consumption to off-line manual sample preparation, which

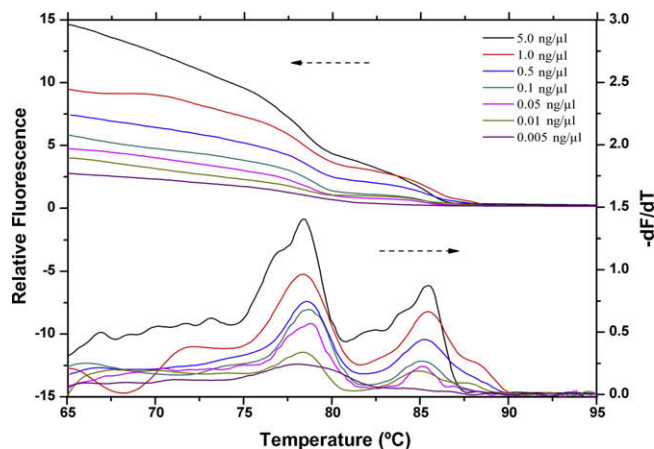


Fig. 9. Fluorescence melting curves for duplex PCR products of the microfluidic device with the different concentrations of the input DNA molecules. The various concentrations of the input DNA molecules were 5.0, 1.0, 0.5, 0.1, 0.05, 0.01, and $0.005 \text{ ng } \mu\text{l}^{-1}$. The amplification was performed at a flow rate of 5.0 mm s^{-1} .

is time-consuming, is poorly portable, and requires multiple laboratory instruments. However, it still takes a long time to perform on-line sample preparation on the PCR microfluidics. Integration with analytical detection, such as capillary electrophoresis followed by laser-induced fluorescence detection, electrochemiluminescent detection, DNA microarray hybridization, and so on could decrease analytical cost, enhance sensitivity and speed of detection, and effectively overcome the errors resulting from some manual operations. Our current efforts are focused on off-line and on-line electrochemiluminescent detection for detecting GMOs [8,10] on this continuous-flow PCR microfluidics. Although the PCR microfluidics provides many advantages over the conventional

PCR device, the miniaturization also raises some challenging issues such as the adsorption of the reagents to the channel surface, the proneness to evaporation of the sample solution and formation of gas bubbles, the requirement of precise temperature control, and so on. Despite these obstacles, the potential of PCR microfluidics as a future nucleic acid amplification is still attractive.

Acknowledgments

This research was supported by the National Natural Science Foundation of China (30700155 and 30600128), the National High Technology Research and Development Program of China (863 Program) (2007AA10Z204), and the Natural Science Foundation of Guangdong Province (7005825).

References

- [1] E. Gachet, G.G. Martin, F. Vigneau, G. Meyer, Detection of genetically modified organisms (GMOs) by PCR: a brief review of methodologies available, *Trends Food Sci. Technol.* 9 (1999) 380–388.
- [2] A. Nadal, A. Coll, J.L. La Paz, T. Esteve, M. Pla, A new PCR–CGE (size and color) method for simultaneous detection of genetically modified maize events, *Electrophoresis* 27 (2006) 3879–3888.
- [3] D. Rodríguez-Lázaro, B. Lombard, H. Smith, A. Rzezutka, M. D'Agostino, R. Helmuth, A. Schroeter, B. Malorny, A. Miko, B. Guerra, J. Davison, A. Kobylinsky, M. Hernández, Y. Bertheau, N. Cook, Trends in analytical methodology in food safety and quality: monitoring microorganisms and genetically modified organisms, *Trends Food Sci. Technol.* 18 (2007) 306–319.
- [4] T. Abdullah, S. Radu, Z. Hassan, J.K. Hashim, Detection of genetically modified soy in processed foods sold commercially in Malaysia by PCR-based method, *Food Chem.* 98 (2006) 575–579.
- [5] A. Holst-Jensen, GMO detection methods and validation review, National Veterinary Institute, Section of Food & Feed Microbiology, Oslo, Norway, 2001.
- [6] G. Ujhelyi, B. Vajda, E. Béki, K. Neszlényi, J. Jakab, A. Jánaosi, E. Némédi, E. Gelencsér, Surveying the RR soy content of commercially available food products in Hungary, *Food Control* 19 (2008) 967–973.
- [7] R.K. Saiki, S. Scharf, F. Faloona, K.B. Mullis, G.T. Horn, H.A. Erlich, N. Arnheim, Enzymatic amplification of β -globin genomic sequences and restriction site analysis for diagnosis of sickle cell anemia, *Science* 230 (1985) 1350–1354.
- [8] T.H. Varzakas, G. Chrysochoidis, D. Argyropoulos, Approaches in the risk assessment of genetically modified foods by the Hellenic Food Safety Authority, *Food Chem. Toxicol.* 45 (2007) 530–542.
- [9] J.F. Liu, D. Xing, X.Y. Shen, D.B. Zhu, Detection of genetically modified organisms by electrochemiluminescence PCR method, *Biosens. Bioelectron.* 20 (2004) 436–441.
- [10] K. Cankar, V. Chauvensy-Ancel, M.N. Fortabat, K. Gruden, A. Kobylinsky, J. Zel, Y. Bertheau, Detection of nonauthorized genetically modified organisms using differential quantitative polymerase chain reaction: application to 35S in maize, *Anal. Biochem.* 376 (2008) 189–199.
- [11] J.F. Liu, D. Xing, X.Y. Shen, D.B. Zhu, Electrochemiluminescence polymerase chain reaction detection of genetically modified organisms, *Anal. Chim. Acta* 537 (2005) 119–123.
- [12] A.J. de Mello, DNA amplification: does “small” really mean “efficient”?, *Lab Chip* 1 (2001) 24–29.
- [13] C.S. Zhang, J.L. Xu, The design development of continuous-flow polymerase chain reaction chip, *Chin. J. Anal. Chem.* 33 (2005) 729–734.
- [14] I. Schneegaß, J.M. Kohler, Flow-through polymerase chain reactions in chip thermocyclers, *Rev. Mol. Biotechnol.* 82 (2001) 101–121.
- [15] H. Nagai, Y. Murakami, K. Yokoyama, E. Tamiya, High-throughput PCR in silicon based microchamber array, *Biosens. Bioelectron.* 16 (2001) 1015–1019.
- [16] M. A. Northrup, M. T. Ching, R. M. White, R. T. Watson, DNA amplification in a microfabricated reaction chamber, in: proceedings of the 7th International Conference on Solid State Sensors and Actuators, Yokohama, Japan, 1993, pp. 924–926.
- [17] H. Nakano, K. Matsuda, M. Yohda, T. Nagamune, I. Endo, T. Yamane, High speed polymerase chain reaction in constant flow, *Biosci. Biotechnol. Biochem.* 58 (1994) 349–352.
- [18] C.S. Zhang, J.L. Xu, W.L. Zheng, PCR microfluidic devices for DNA amplification, *Biotechnol. Adv.* 24 (2006) 243–284.
- [19] C.S. Zhang, D. Xing, Miniaturized PCR chips for nucleic acid amplification and analysis: latest advances and future trends, *Nucleic Acids Res.* 35 (2007) 4223–4237.
- [20] C.S. Zhang, D. Xing, Y.Y. Li, Micropumps, microvalves, and micromixers within PCR microfluidic chips: advances and trends, *Biotechnol. Adv.* 25 (2007) 483–514.
- [21] J.G. Lee, K.H. Cheong, N. Huh, S. Kim, J.W. Choi, C. Ko, Microchip-based one step DNA extraction and real-time PCR in one chamber for rapid pathogen identification, *Lab Chip* 6 (2006) 886–895.
- [22] R. Prakash, K.V.I.S. Kaler, An integrated genetic analysis microfluidic platform with valves and a PCR chip reusability method to avoid contamination, *Microfluid. Nanofluid.* 3 (2007) 177–187.
- [23] B.C. Giordano, J. Ferrance, S. Swedberg, A.F.R. Hühmer, J.P. Landers, Polymerase chain reaction in polymeric microchips: DNA amplification in less than 240 seconds, *Anal. Biochem.* 291 (2001) 124–132.
- [24] J. Liu, M. Enzelberger, S. Quake, A nanoliter rotary device for polymerase chain reaction, *Electrophoresis* 23 (2002) 1531–1536.
- [25] C.S. Zhang, J.L. Xu, J.Q. Wang, H.P. Wang, Experimental study of continuous-flow polymerase chain reaction microfluidics based on polytetrafluoroethylene capillary, *Chin. J. Anal. Chem.* 34 (2006) 1197–1202.
- [26] P.A. Auroux, Y. Koc, A. deMello, A. Manz, P.J. Day, Miniaturized nucleic acid analysis, *Lab Chip* 4 (2004) 534–546.
- [27] J. West, M. Becker, S. Tombrink, A. Manz, Micro total analysis systems: latest achievements, *Anal. Chem.* 80 (2008) 4403–4419.
- [28] M.U. Kopp, A.J. de Mello, A. Manz, Chemical amplification: continuous-flow PCR on a chip, *Science* 280 (1998) 1046–1048.
- [29] K. Sun, A. Yamaguchi, Y. Ishida, S. Matsuo, H. Misawa, A heater-integrated transparent microchannel chip for continuous-flow PCR, *Sens. Actuat. B* 84 (2002) 283–289.
- [30] P.J. Obeid, T.K. Christopoulos, H.J. Crabtree, C.J. Backhouse, Microfabricated device for DNA and RNA amplification by continuous-flow polymerase chain reaction and reverse transcription–polymerase chain reaction with cycle number selection, *Anal. Chem.* 75 (2003) 288–295.
- [31] J.H. Liu, X.F. Yin, G.M. Xu, Z.L. Fang, H.Z. Chen, Studies on a microfluidic chip based on the continuous flow PCR amplification system, *Chem. J. Chin. Univ.* 24 (2003) 232–235.
- [32] L.Y. Yao, B.A. Liu, T. Chen, S.B. Liu, T.C. Zuo, Micro flow-through PCR in a PMMA chip fabricated by KrF excimer laser, *Biomed. Microdevices* 7 (2005) 253–257.
- [33] J.A. Kim, J.Y. Lee, S. Seong, S.H. Cha, S.H. Lee, J.J. Kim, T.H. Park, Fabrication and characterization of a PDMS–glass hybrid continuous-flow PCR chip, *Biochem. Eng. J.* 29 (2006) 91–97.
- [34] M. Hashimoto, F. Barany, F. Xu, S.A. Soper, Serial processing of biological reactions using flow-through microfluidic devices: coupled PCR/LDR for the detection of low-abundant DNA point mutations, *Analyst* 132 (2007) 913–921.
- [35] M. Curcio, J. Roeraade, Continuous segmented-flow polymerase chain reaction for high-throughput miniaturized DNA amplification, *Anal. Chem.* 75 (2003) 1–7.
- [36] N. Park, S. Kim, J.H. Hahn, Cylindrical compact thermal-cycling device for continuous-flow polymerase chain reaction, *Anal. Chem.* 75 (2003) 6029–6033.
- [37] M. Hashimoto, P.C. Chen, M.W. Mitchell, D.E. Nikitopoulos, S.A. Soper, M.C. Murphy, Rapid PCR in a continuous flow device, *Lab Chip* 4 (2004) 638–645.
- [38] J.H. Liu, X.F. Yin, Z.L. Fang, Automatic continuous amplification of long fragments DNA with spiral flow through PCR microchip, *Chem. J. Chin. Univ.* 25 (2004) 30–34.
- [39] K.D. Dorfman, M. Chabert, J.H. Codarbox, G. Rousseau, P. de Cremoux, J.L. Viovy, Contamination-free continuous flow microfluidic polymerase chain reaction for quantitative and clinical applications, *Anal. Chem.* 77 (2005) 3700–3704.
- [40] C.S. Zhang, J.L. Xu, J.Q. Wang, H.P. Wang, Continuous-flow polymerase chain reaction microfluidics by using spiral capillary channel embedded on copper, *Anal. Lett.* 40 (2007) 497–511.
- [41] C.S. Zhang, D. Xing, J.L. Xu, Continuous-flow PCR microfluidics for rapid DNA amplification using thin film heater with low thermal mass, *Anal. Lett.* 40 (2007) 1672–1685.
- [42] J. Chiou, P. Matsudaira, A. Sonin, D. Ehrlich, A closed-cycle capillary polymerase chain reaction machine, *Anal. Chem.* 73 (2001) 2018–2021.
- [43] P. Belgrader, C.J. Elkin, S.B. Brown, S.N. Nasarabadi, R.G. Langlois, F.P. Milanovich, B.W. Colston, G.D. Marshall Jr., A reusable flow-through polymerase chain reaction instrument for the continuous monitoring of infectious biological agents, *Anal. Chem.* 75 (2003) 3446–3450.
- [44] W. Wang, Z.X. Li, R. Luo, S.H. Lü, A.D. Xu, Y.J. Yang, Droplet-based micro oscillating-flow PCR chip, *J. Micromech. Microeng.* 15 (2005) 1369–1377.
- [45] J.Y. Cheng, C.J. Hsieh, Y.C. Chuang, J.R. Hsieh, Performing microchannel temperature cycling reactions using reciprocating reagent shuttling along a radial temperature gradient, *Analyst* 130 (2005) 931–940.
- [46] M. Hernández, D. Rodríguez-Lázaro, T. Esteve, S. Prat, M. Pla, Development of melting temperature-based SYBR Green I polymerase chain reaction methods for multiplex genetically modified organism detection, *Anal. Biochem.* 323 (2003) 164–170.
- [47] R.H. Lekan Deprez, A.C. Fijnvandraat, J.M. Ruijter, A.F.M. Moorman, Sensitivity and accuracy of quantitative real-time polymerase chain reaction using SYBR Green I depends on cDNA synthesis conditions, *Anal. Biochem.* 307 (2002) 63–69.
- [48] K.M. Ririe, R.P. Rasmussen, C.T. Wittwer, Product differentiation by analysis of DNA melting curves during the polymerase chain reaction, *Anal. Biochem.* 245 (1997) 154–160.
- [49] K.S. Elenitoba-Johnson, S.D. Bohling, C.T. Wittwer, T.C. King, Multiplex PCR by multicolor fluorimetry and fluorescence melting curve analysis, *Nat. Med.* 2 (2001) 249–253.
- [50] W. Fan, T. Hamilton, S. Webster-Sesay, M.P. Nikolich, L.E. Lindler, Multiplex real-time SYBR Green I PCR assay for detection of tetracycline efflux genes of gram-negative bacteria, *Mol. Cell Probes* 21 (2007) 245–256.
- [51] K.M. Remund, D.A. Dixon, D.L. Wright, L.R. Holden, Statistical considerations in seed purity testing for transgenic traits, *Seed Sci. Res.* 11 (2001) 101–119.
- [52] A. Kobylinsky, Y. Bertheau, Minimum cost acceptance sampling plans for grain control, with application to GMO detection, *Chemometr. Intell. Lab. Syst.* 75 (2005) 189–200.